Carbohydrate Polymers 105 (2014) 351–358

Contents lists available at ScienceDirect

Carbohydrate Polymers

journal homepage: www.elsevier.com/locate/carbpol

Preparation and characteristics of sodium alginate/Na$^+$rectorite-g-itaconic acid/acrylamide hydrogel films

Lianli Yang [a,*], Xiaoyan Ma [b], Naini Guo [a], Yang Zhang [a]

[a] College of chemistry and chemical engineering, Xianyang Normal University Xianyang, Shaanxi 712000, PR China
[b] Department of Applied Chemistry, School of Science Northwestern Polytechnical University Xi'an, Shaanxi 710072, PR China

ARTICLE INFO

Article history:
Received 24 November 2013
Accepted 12 January 2014
Available online 31 January 2014

Keywords:
SA/Na$^+$REC-g-IA/AM
Hydrogel film
Preparation
Characteristics
Salicylic acid
Controlled release

ABSTRACT

Sodium alginate/Na$^+$rectorite-graft-itaconic acid/acrylamide (SA/Na$^+$REC-g-IA/AM) hydrogel film was prepared via solution polymerization. The effect of Na$^+$REC, KPS, and NMBA content and the ratio of IA to AM on graft ratio, graft efficiency and absorption of liquids were investigated. The structure and morphology were analyzed by FTIR, XRD, TEM and SEM. Results revealed that the optimal Na$^+$REC, KPS, and NMBA content and the ratio of IA to AM were 2 wt%, 0.8 wt%, 0.38 wt% and 4, respectively. The hydrogel film was found to exhibit an intercalative structure and coarse surface. The mechanism of graft copolymerization was discussed. A slower and more continuous release of salicylic acid for SA/Na$^+$REC-g-IA/AM composite hydrogel film was shown in vitro drug-controlled release studies, in comparison with SA film. The salicylic acid release mechanism of SA/Na$^+$REC-g-IA/AM hydrogel film followed Fickian diffusion.

1. Introduction

Hydrogel, soft and pliable, is a three-dimensional macromolecular network with the ability to absorb and retain large amounts of water without dissolution when immersed in water or biological fluids (Montero et al., 2012; Bunsow & Johannsmann, 2008; Mandal, Ghosh, & Kundu, 2011). Their water retaining capacity and good biocompatibility makes them important materials in chemical sensors (Bunsow & Johannsmann, 2008; Montero et al., 2012; Mandal et al., 2011; Shen & He, 2007), bioanalytics (Smitha, Sridha, & Khan, 2005), tissue engineering (Wang, Sabina, Du, & Vårum, 2010), particular relevance on pharmaceutical and biomedical applications (Ding, He, Zhou, Tang, & Yin, 2012; Deligkaris et al., 2010; Kokabi et al., 2007; Pereira et al., 2013; Wang et al., 2007; Yue, Sheng, & Wang, 2009). Hydrogel normally includes synthetic, semi-synthetic and natural polymers. Although synthetic hydrogels have large water absorbing capacities, the consumed polymers have led to serious environmental pollution. Growing environmental concerns have created an urgent need to develop natural polymers due to their low cost, low toxicity, bio-degradability and environmental-friendly nature (Lanthong, Nuisin, & Kiatkamjornwong, 2006; Li, Zhang, & Wang, 2007 ; Mandal et al., 2011; Roy et al., 2012; Pereira et al., 2013; Takikawa et al., 2010; Yoshimura, Uchikoshi, Yoshiura, Fujioka, 2005; Zhao et al., 2009; Zhou & Wu, 2011). Murakami et al. 2010 prepared a composite hydrogel sheet composed of alginate, chitin/chitosan and fucoidan (ACF-HS) produced from blended powder. ACF-HS is an excellent wound dressing for the repair of healing-impaired wounds. Carboxymethyl chitosan oligosaccharide/rectorite hydrogel film was prepared by microwave irradiation by Liu et al., 2012, and its inhibitory activity against microorganisms was strong.

Sodium alginate (SA) is a kind of polysaccharide in nature, which is mainly composed of (1–4)-linked β-D-mannuronic acid units and α-L-guluronic acid units (Teli, Gokavi, & Aminabhavi; Yang, Liang, Zhang, He, & Wang, 2009), and can be arranged in the form of homopolymeric sequences (MMM or GGG) or alternating sequences (MGMG) along the polymeric chain (Smitha et al., 2005). The alginate physical, chemical and gelling properties are strongly determined by the content of M and G blocks (Yang, Ma, & Guo, 2012; Yang et al., 2009). The gelling property, relative low cost, biocompatibility, nontoxicity and biodegradability of sodium alginate suggest that it would have potential applications as medical materials, sanitary materials, tissue engineering materials, controlled-release devices and matrices for enzyme immobilization, etc (Pereira et al., 2013; Smitha et al., 2005; Pongjanyakul et al., 2010; Teli et al., 2007; Yang et al., 2012). Several reports have suggested that certain alginate dressings can enhance wound healing by stimulating monocytes to produce elevated levels of cytokines (Balakrishnan et al., 2005; Murakami et al., 2010).

Rectorite, as a type of layered materials, which has similar structure to montmorillonite, is easily available in China. In addition, rectorite exhibits good mechanical and thermal properties as well as high resistance to ultraviolet ray, etc. A single rectorite layer has a thickness of ~2 nm, while its width and length vary from one

* Corresponding author: Tel.: +86 29 33720704; fax: +86 29 33720704.
E-mail address: lianli1968@163.com (L. Yang).

0144-8617/$ – see front matter © 2014 Elsevier Ltd. All rights reserved.
http://dx.doi.org/10.1016/j.carbpol.2014.01.043

micron to several microns (Yoshimura et al., 2005). The interlayer cations of rectorite layers can be exchanged easily by either organic or inorganic cations, thus making it possible to prepare polymer/rectorite nanocomposites. Researches on polymer/rectorite nanocomposites have been carried out, and results show that the addition of rectorite can endow polymers with higher mechanical, thermal, and anti-ultraviolet properties, etc (Wang et al., 2007, 2010; Wang, & Wang, 2009; Yang et al., 2009). Natural rectorite clay normally contains pyrites, which affect rectorite's application performance, for instance, by hindering graft copolymerization reaction of monomers and polysaccharide in the interlayer of rectorite. So pyrites were removed by calcination in this context. Meanwhile, the white degree of rectorite was also improved by calcination. On the other hand, there are many Ca^{2+}, Mg^{2+}, Al^{3+} in the interlayer of natural rectorite, forming the polycrystalline layer which is difficult to be exfoliated. Moreover, Ca^{2+}, Mg^{2+}, Al^{3+} hindered the intercalation of sodium alginate and monomers in the interlayer of rectorite. So calcination rectorite was modified with sodium pyrophosphate to obtain Na^+Rectorite (Na^+REC). The results showed that the d_{001} values of Na^+REC is larger than natural rectorite (Yang et al., 2009, 2012).

As an extension of our previous work on SA/Na^+REC composite film (Yang et al., 2009), a nontoxic, biocompatible and biodegradable hydrogel film was synthesized based on SA/Na^+REC composite, itaconic acid and acrylamide by solution polymerization. The main factors affecting the preparation of sodium alginate/Na^+rectorite-g-itaconic acid/acrylamide hydrogel have been discussed. The hydrogel film was then subjected to characterisation analysis and mechanical properties. This hydrogel film was also successfully loaded with salicylic acid, and salicylic acid release behavior of the hydrogel film was studied. This hydrogel film provides promising applications as chemical sensors, bioanalytics, tissue engineering, drug delivery and wound dressing, etc.

2. Experimental

2.1. Materials

SA was obtained from Kemiou Chemical Co. Ltd. (Tianjing, China). REC was purchased from Hubei Zhongxiang Rectorite Mine (Wuhan, China), with cationic exchange capacity (CEC) 45 meq/100 g, and d-space value 2.1225 nm. Itaconic acid was made at Tianjin Standard Science and Technology Co. Ltd. (Tianjing, China). Acrylamide was supplied by at Shanghai Wulian Chemical Factory (Shanghai, China). Sodium pyrophate was purchased from Tianjin Boddy Chemical Co. Ltd. (Tianjing, China). Glycerine was obtained from Tianjin Daqiuzhuang Froth Plastics plant (Tianjing, China). Potassium persulphate (KPS, analytical grade) was produced by Xi'an Chemical Reagent Factory (Xi'an, China). *N,N'*-methylene-bisacrylamide (NMBA, chemical grade) was made by Shanghai Chemical Reagent Corporation (Shanghai, China). Salicylic acid was purchased from Beijing Tianqin Yihe Biological Technology Co. Ltd. (Beijing, China).

2.2. Synthesis of Na^+REC

REC was calcined in Muffle furnace (Model MF-900, Nanjing University Instrument Plant, Nanjing, China) at 850 °C for 4 h to increase its white degree and improve its activity (Yang et al., 2009, 2012). The synthesis of Na^+REC includes the following steps. Firstly, 10.0 g of calcined REC was dissolved in deionized water to obtain 15 wt% suspension solution. Secondly, 0.3 g sodium pyrophate was added into the suspension with stirring and maintained at the condition for 0.5 h to obtain a mixture. Thirdly, the mixture was slowly heated to 60 °C and maintained at that temperature for 12 h. At last, the mixture was cooled to 30 °C; then it was filtered by a Buncher filter and dried. The product is coded as Na^+REC.

2.3. Preparation of SA/Na^+REC-g-itaconic acid/acrylamide hydrogel films

Firstly, Na^+REC and distilled water were put into a 250 ml three-necked flask equipped with a stirrer, a condenser and a nitrogen line to obtain 3 wt% suspension liquid. SA was dissolved in deionized water to form a homogeneous solution of 3 wt% polysaccharide. Secondly, SA solution was slowly mixed into Na^+REC suspension liquid; then the plasticizer glycerine (10% w/w based on SA) was dropped into the mixture. The mixture was stirred with a high speed shear mixer for 3 h. Thirdly, KPS, itaconic acid which was partially neutralized by adding 40 wt% NaOH solution (mass percent) and a weight quantity of AM were added after the oxygen was ejected completely by a nitrogen flow. The grafting reaction was carried out for 3 h at a temperature of 80 °C. Fourthly, the cross-linker (NMBA) was added into the solution by stirring for 0.5 h. The crude product salivated on a dust-free glass plate with a uniform thickness for curing by a procedure of 60 °C for 5 h. After curing, dried membrane was peeled off from the glass plate. The resultant film is designed as SA/Na^+REC-g-IA/AM hydrogel film. The average thickness of the samples was 0.08 mm.

2.4. Measurements

The hydrogel film was extracted in a Soxhlet's extractor with 80% acetone solution for 24 h. The extracted product was dried in a vacuum oven at 65 °C for 24 h and weighed to determine the amounts of the graft copolymer. The grafting ratio (%*G*) and grafting efficiency (%*E*) were calculated by using the following formulas:

$$G(\%) = \left(\frac{W_2}{W_0}\right) \times 100\% \quad (1)$$

$$E(\%) = \left(\frac{W_2}{W_1}\right) \times 100\% \quad (2)$$

where W_0, W_1, and W_2 denote the weight of SA, crude hydrogel product and graft copolymer, respectively.

The swelling rate (Q) of hydrogel was measured by the following procedure: a weighted quantity of the hydrogel films was immersed in distilled water or 0.9 wt% NaCl solutions at room temperature to reach the swelling equilibrium. Swollen samples were then separated from unabsorbed water by filtering over a 300-mesh screen. The swelling rate (Q) of hydrogel film was calculated by using Eq. (3):

$$Q = \frac{m_2 - m_1}{m_1} \quad (3)$$

where m_1 is the weight of dry sample, and m_2 is the weight of water-swollen sample.

The structures of superabsorbent composite were investigated using DPmax23C X-ray diffraction (XRD) instrument (Rigaku, Osaka, Japan) with Cu K_α ($\lambda = 0.154$ nm) radiation source. The X-ray generator operated at 35 kV and 50 mA, the reflection angle 2θ was monitored from 2.0° to 12.5° at a scanning speed of 2°/min and a step size of 0.02°.

FTIR spectra of purified hydrogel films were recorded with KBr pellets on a Fourier transform infrared spectrometer (Model VECTOR-22, Shimazu, Kyoto, Japan).

The exfoliation and molecular dispersion of clay layers in nanocomposites were observed using a Hitachi H-800 transmission electron microscopy (TEM) instrument (Hitachi, Japan) with an acceleration voltage of 150 kV, and the ultra-thin samples with a thickness of less than 1 μm were microtomed in liquid nitrogen using LKB Bromma 2088 cutter.

The morphology of product was observed using scanning electron microscopy (SEM) (KYKY1000B, Scientific Instrument Factory CAS, Beijing, China). Prior to observation, samples were arranged on metal grids by using double-sided adhesive tape; in addition, samples were coated with gold under vacuum.

The tensile strength and the percentage of elongation at break for SA/Na$^+$REC-g-IA/AM hydrogel films were determined on testing machine, Model PT-1036PC (Chengde, China). The films were cut into 15 cm × 1 cm strips. The gauge length was 50 mm, and the crosshead speed was 50 mm/min.

2.5. Salicylic acid adsorption and release in vitro

The adsorption experiments of hydrogel films to salicylic acid were carried out in 250 ml Erlenmeyer flasks equipped with stoppers, which contains 0.1000 g absorbent, i.e., SA/Na$^+$REC-g-IA/AM hydrogel film and 100 ml, 50% ethanol aqueous salicylic acid solutions with an initial concentration of 500 mg/L. The mixtures were vigorously stirred for 12 h at 298 K. The salicylic acid solutions were separated from the adsorbents. The absorbency of the solutions was determined with a UV–visible spectrophotometer (UV-265FW, Shimadzu Corp. (Kyoto, Japan)) at λ = 298 nm. The absorbency (mg/g) was calculated according to Eq. (4):

$$\text{absorbency} = \frac{V(c_0 - c_1)}{m} \quad (4)$$

where c_0 is the initial solution concentration (mg/L), c_1 is the final solution concentration (mg/L), V is the solution volume (L), and m is the mass of the absorbent (g).

The drug-loaded films were immersed in 50 ml aliquots of 0.1 M sodium phosphate buffer containing 0.85% sodium chloride, pH 7.4 (PBS), and incubated on a constant temperature shaking bed at 37 °C and 130 rpm. After specific intervals, 1 ml aliquot of samples were withdrawn and immediately replaced with the same amount of fresh medium.

3. Results and discussion

3.1. Mechanism of graft

SA/Na$^+$REC intercalated nanocomposite was prepared via a solution-mixing processing technique. The swollen silicate layers of Na$^+$REC are exfoliated into SA matrix depending on two processes, namely, SA chain intercalation into clay galleries, and nano clay layers exfoliation under shearing force. The sum of van der Waals force and electrostatic attractive force against clay exfoliation, while the shearing force and elastic force arising due to SA molecular intercalation favor clay exfoliation (Monvisade & Siriphannon, 2009; Yang et al., 2009). There is a strong intermolecular hydrogen bonding interface between active hydroxyl on the surface of Na$^+$REC and carboxyl of SA.

Graft copolymerization of itaconic acid and acrylamide onto the backbone of SA/Na$^+$REC composite by initiator attributes to free radical reaction. The mechanism for polymerization process is shown in Fig. 1. The whole process includes chain initiation, graft and crosslinking. Firstly, peroxysulfate ion serves as a thermally dissociated initiator. It is readily dissociated to $SO_4^{-\bullet}$ and then the radicals attack sodium alginate, leading to the breakage of C—H bond to form SA-based radical (Yang et al., 2012). Then, it will react with itaconic acid and acrylamide molecule, followed by propagation, which leads to growth of a branched chain. *N,N'*-methylene bisacrylamide has two double bonds that can contribute to the crosslinking reaction (Yang et al., 2012; Zhao et al., 2008). The crosslinking formation can be carried out in two ways: (a) the radicals on graft copolymer result in active centers capable of initiating free radical reactions with *N,N'*-methylene bisacrylamide; (b) self-crosslinking of the free radicals onto graft copolymer results in crosslink points. At the same time, Na$^+$REC clay mineral particle in network also acts as crosslinking point, which will cause the formation of an additional network. These reactions would lead to the formation of poly itaconic acid coacrylamide grafted onto sodium alginate/Na$^+$REC composite.

3.2. Effect of Na$^+$REC, KPS, NMBA content and the ratio of IA to AM on the graft copolymerization

Fig. 2a–d shows the influence of Na$^+$REC, KPS, NMBA contents and the ratio of IA to AM on the grafting ratio, grafting efficiency, water and 0.9% NaCl absorption of SA/Na$^+$REC-g-IA/AM hydrogel film. As can be seen from Fig. 2a, the grafting ratio, grafting efficiency, water and 0.9% NaCl absorption of the hydrogel film increase with increasing Na$^+$REC content first, and then decrease with further increasing of Na$^+$REC after reaching 2 wt% (based on sodium alginate). This is because, at low concentration, Na$^+$REC is well dispersed in the SA matrix and exfoliated to be a single layered sheet so that SA and monomers can be intercalation into layers of Na$^+$REC, and then enhance graft copolymerization. Furthermore the hydroxyl group present in Na$^+$REC may react with the KPS and liberate a free radical on Na$^+$REC structure, and graft polymerization will take place on these free radicals giving SA-g-IA/AM branches on Na$^+$REC backbone, which could improve the polymeric network. However, the aggregation of Na$^+$REC clusters at higher Na$^+$REC content causes the grafting ratio, grafting efficiency and absorption of hydrogel film decrease. At the same time, Na$^+$REC clay mineral particle in the network, acted as crosslinking point, which caused the formation of an additional network and decreased the available free volume within the hydrogel film, and then the osmotic pressure difference decreased.

Kalium persulphate (KPS) was used as the initiator in the preparation. Initially, more content of KPS leads to high grafting ratio, grafting efficiency and water and 0.9% NaCl adsorption of SA/Na$^+$REC-g-IA/AM hydrogel film. However, they start to decline when the KPS content is higher than 0.8 wt% (based on monomers). This could be explained by the fact that the initiator is mostly utilized in producing a large number of free-radical sites on SA, Na$^+$REC and monomers. When the KPS content increases, the system produces more active center. However, the excessive increase in the concentration of KPS produced free radical species from the decomposition of KPS to give the termination reaction with sodium alginate macroradicals or a combination reaction between them, which in turn resulted in an increase in soluble materials at fixed crosslinking density. Consequently, the grafting ratio, grafting efficiency and adsorption decreased.

N,N'-methylene bisacrylamide (NMBA) was used as the cross-linker in the preparation. When the crosslinking agent dosage was lower than 0.38 wt% (based on monomers), the grafting ratio, grafting efficiency and water and 0.9% NaCl adsorption increased with further increasing the ratio. However, they began to decrease with the increasing cross-linker content when it was higher than 0.38 wt%. The reason lies in the crosslinking reaction which takes place through any site in growing polymer chains and opening the double bonds of the two vinyl groups of the crosslinker; however, the free polymer contents decrease with the increasing amount of crosslinker because the majority of the monomers were used up in the crosslinking copolymerization, which decreased the residue monomer concentration in the graft copolymerization.

It can be seen from Fig. 2d that the grafting ratio, grafting efficiency and water and 0.9% NaCl adsorption increased with further increasing the ratio, when the ratio of IA to AM was lower than 4. However, they began to decrease with further increased ratio, higher than 4. The reason is that IA is double fold increase, and its reactivity is higher than AM, which render that the structure of

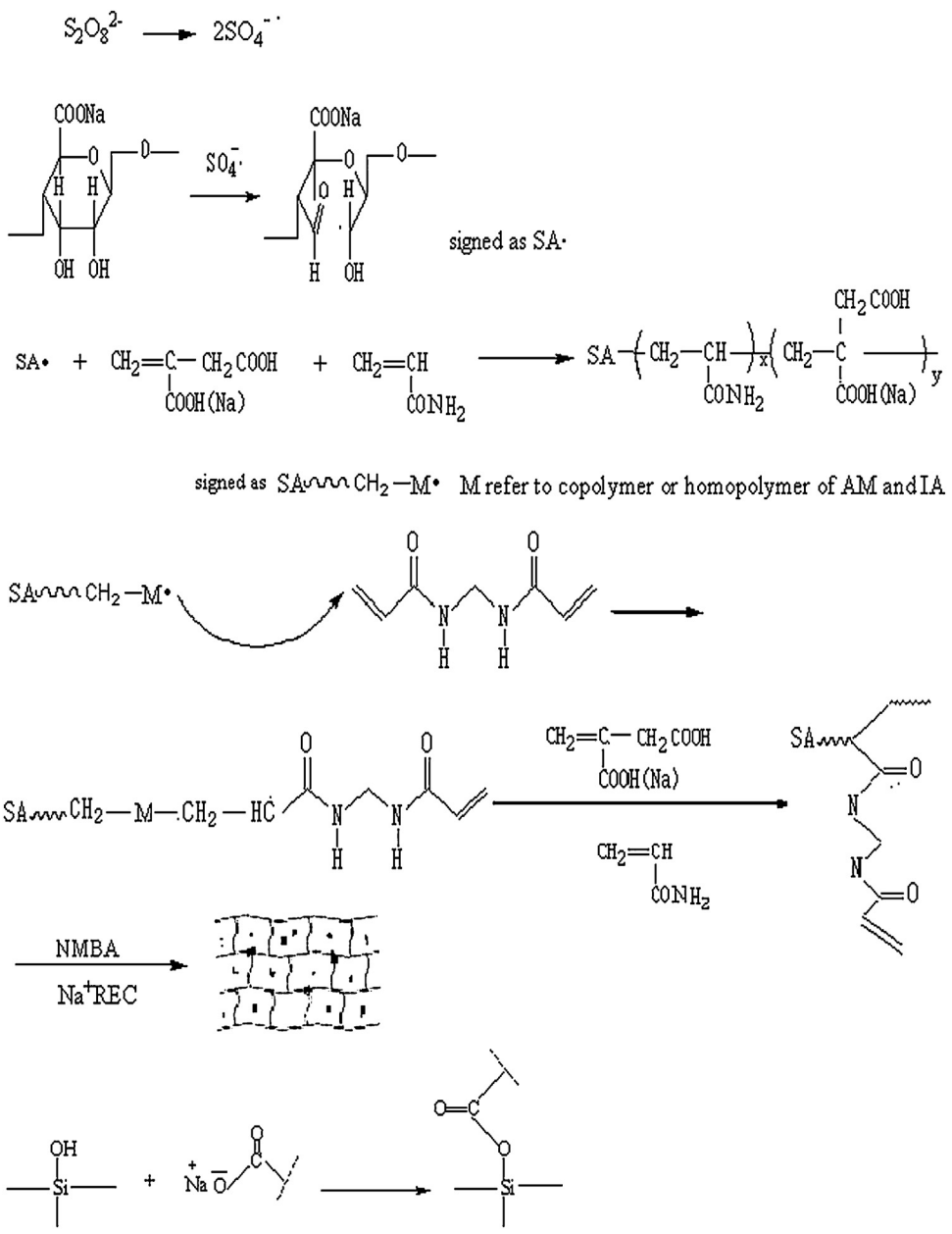

Fig. 1. Scheme of graft-copolymerization of SA, IA, AM and Na^+REC.

the graft copolymer should contain more IA units than AM units, and hydrophilicity of IA is higher than that of AM (Lanthong et al., 2006). Nevertheless, itaconic acid is a diprotic vinyl monomer having two polar groups, which prefer to homopolymerizing rather than becoming a grafted copolymer onto SA backbone. Moreover, acrylamide is a nonionic monomer, which can improve hydrogel salt tolerance.

So the optimal conditions were found as the amount of Na^+REC was 2 wt%, the amount of KPS was 0.8%, the amount of NMBA was 0.38% and the optimal ratio of IA to AM was 4.

3.3. Structure and morphology of SA/Na^+REC-g-IA/AM hydrogel film

Fig. 3 shows FTIR spectra of Na^+REC, SA and SA/Na^+REC-g-IA/AM. For Na^+REC, 3431 cm^{-1} is attributed to the bending vibration of hydrogen band of interlaminar water in Na^+REC, 3632 cm^{-1} is attributed to the hydroxyl stretching of SiOH, 1639 cm^{-1} represents hydroxyl bending of H_2O, 1050 cm^{-1} is associated with the anisomerous stretching vibration of Si—O—Si, 450–550 cm^{-1} is attributed to the bending vibration of Si—O (Bardajee, Pourjavadi, Soleyman, Sheikh, 2008; Li et al., 2008). 927 cm^{-1} is the stretching vibration of P—O of sodium pyrophosphate(Yang et al., 2012). The IR spectrum of alginate shows absorption bands at 3430 cm^{-1} (OH stretching), 1618 cm^{-1} (COO^- asymmetric stretching), and 1410 cm^{-1} (COO^- symmetric stretching). By comparison with the infrared spectra of SA and SA/Na^+REC-g-IA/AM composite, the strong absorption peak at 1030 cm^{-1} is attributed to vibration of the hydroxyl on cyclic alcohols of SA disappears, suggesting that the ring of SA was opened in the reaction (Fig. 1). Twin peaks at 1638 and 1650 cm^{-1} appear in the spectrum of SA/Na^+REC-g-IA/AM, indicating the existence of C=O of IA and AM(Lanthong et al., 2006). Additionally, the peaks found at 3400, 1650, and 1372 cm^{-1} indicate the N—H stretching, the C=O stretching and N—H bending of the amide bands, respectively, which are characteristics of the $-CONH_2$ group in the acrylamide(Bardajee et al., 2008). The

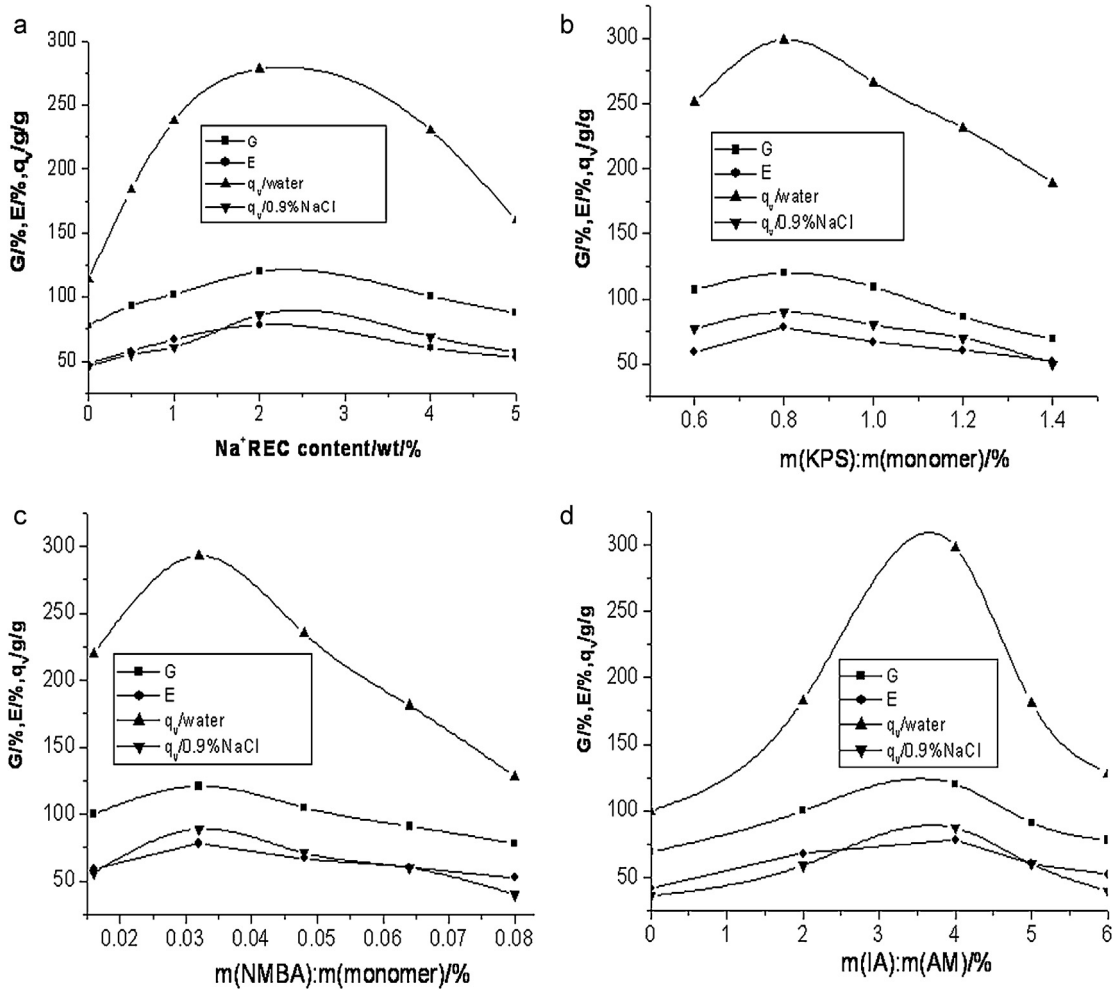

Fig. 2. Effect of Na^+REC, KPS, NMBA contents and the ratio of IA to AM on the graft copolymerization.
(a effect of Na^+REC content on the graft copolymerization; b effect of KPS content on the graft copolymerization; c effect of NMBA content on the graft copolymerization; d effect of the ratio of IA to AM on the graft copolymerization.)

broad peak at 3400–3600 cm^{-1} (—OH), 1600 and 1410 cm^{-1} of symmetric and asymmetric —COO— stretching absorption bands appear in the spectrum of SA/Na^+REC-g-IA/AM, indicating the existence of —COOH (Lanthong et al., 2006). Comparing with Na^+REC, the intensity of the absorption bands at 3431 cm^{-1} ascribing to the bending vibration of —OH increases in the spectrum

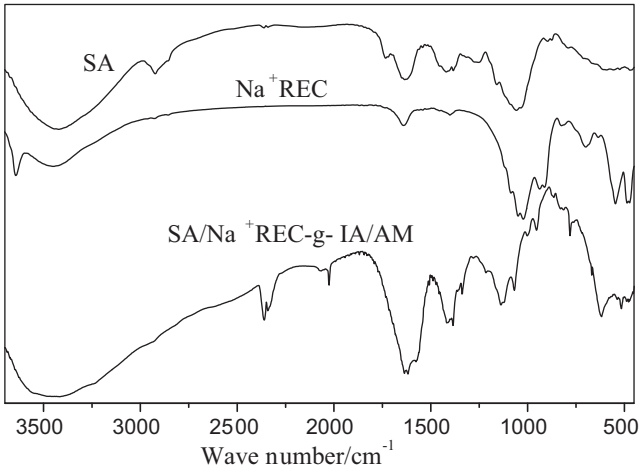

Fig. 3. FTIR spectra of Na^+REC, SA and SA/Na^+REC-g-IA/AM composite.

of SA/Na^+REC-g-IA/AM, and the absorption band at 3616 cm^{-1} of Na^+REC disappears, implying that the —OH groups on Na^+REC participate in the reaction. 1042 cm^{-1} assigned to the anisomerous stretching vibration of Si—O—Si, 550 cm^{-1} assigned to the bending vibration of Si—O slightly shifted to a low wave number and the peak intensity reduced. The IR analysis results indicated that the graft copolymerization of IA and AM on both Na^+REC and SA took place during polymerization process and the resulting product was a composite based on P(IA-co-AM) incorporating with Na^+REC and SA.

Fig. 4 shows XRD patterns of Na^+REC, SA and SA/Na^+REC-g-IA/AM. The XRD pattern of SA shows that SA exhibits an amorphous structure. The XRD pattern of the Na^+REC shows a reflection peak at about $2\theta = 4.0$, corresponding to a basal spacing (d 0 0 1) of 2.2073nm. It can be observed from Fig. 4 that the (0 0 1) plane diffraction peaks of SA/Na^+REC-g-IA/AM composites are shifted slightly to lower angle and have weaker (0 0 1) plane reflection peaks than Na^+REC, indicating that intercalation is formed between Na^+REC and polymer matrix. The conclusion can be confirmed by TEM micrograph.

Fig. 5 gives TEM micrograph magnified ten thousand times of SA/Na^+REC-g-IA/AM composite hydrogel, in which the gray areas represent the silicate layers in the polymer matrix (bright). The clay mineral platelets were well dispersed into matrix without agglomerations of platelets so that an intercalative/exfoliated structure was obtained, as observed from the TEM results.

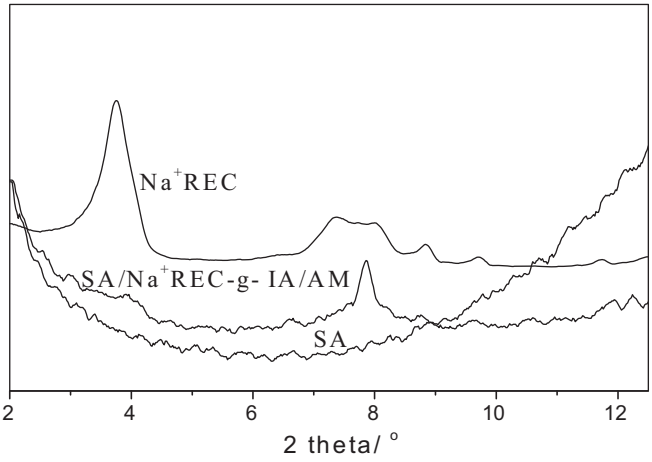

Fig. 4. X-ray diffraction patterns of Na^+REC, SA and SA/Na^+REC-g-IA/AM hydrogel.

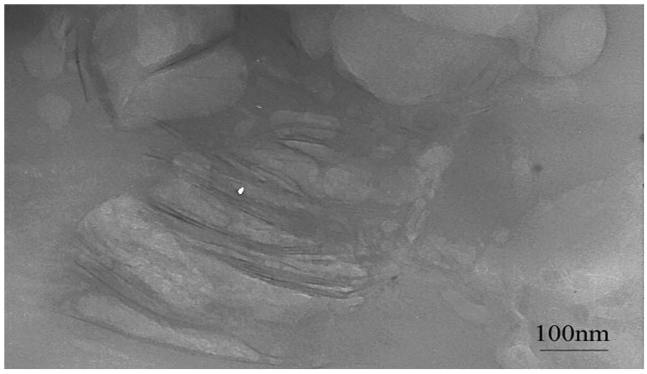

Fig. 5. TEM analysis of SA/Na^+REC-g-IA/AM composite hydrogel (100,000 times).

Fig. 6a and b gives SEM photos of SA/Na^+REC-g-IA/AM hydrogel film obtained at different magnifications. Fig. 6b showed that SA/Na^+REC-g-IA/AM hydrogel film exhibited a three-dimensional network structure and coarse surface. This surface structure facilitates the permeation of water and drug. Fig. 6b also showed SA/Na^+REC-g-IA/AM hydrogel had intercalative nanostructure, in which the bright areas represent the silicate layers in the SA-g-IA/AM matrix (gray). This means that the hydrogel film could present good mechanical and thermal properties, etc.

3.4. Tensile strength and elongation at break

An ideal wound dressing should present good mechanical properties and maintain their integrity during use. Meanwhile, the films should possess adequate resistance to the mechanical abrasion and be flexible to follow the skin movements. The tensile strength and elongation value of SA/Na^+REC-g-IA/AM hydrogel film obtained from optimum conditions have been investigated and results are listed in Table 1. The tensile strength and elongation value of SA/Na^+REC-g-IA/AM dry hydrogel film are 15.3 MPa and 62.3%, respectively, which increase 36.6% and 84.9% comparing with pure SA film (SA film was immersed for 15 min in a 1% (w/v) tripolyphosphate solution to crosslink). The SA/Na^+REC-g-IA/AM film present higher malleability and a very smooth surface when immersed in distilled water for 12 h. The tensile strength and elongation value of SA/Na^+REC-g-IA/AM wet hydrogel film are 5.70 MPa and 30.6%, respectively, which demonstrates a 147.8% and 128.4% improvement, respectively, compared to wet SA film. The value of the tensile strength of the skin is usually in the range 2.5–16 MPa, and the elongation is approximately 70% in the most flexible zones (Kokabi et al., 2007; Murakami et al., 2010). Comparing theses values with the mechanical properties of SA/Na^+REC-g-IA/AM hydrogel film, it demonstrates adequate properties for skin application.

3.5. Salicylic acid adsorption and release in vitro studies

As a monohydroxybenzoic acid, salicylic acid from willow tree is known for its ability to ease aches and pains and reduce fevers. These medicinal properties make it as an anti-inflammatory drug. Salicylic acid was used as a model drug to investigate the drug adsorption and release from SA/Na^+REC-g-IA/AM hydrogel film. The adsorption results showed SA film has lower adsorption capacities for salicylic acid than SA/Na^+REC-g-IA/AM hydrogel film. Its absorbency for salicylic acid is 18.8 mg/g. The absorbency of SA/Na^+REC-g-IA/AM films increased to 55.7 mg/g. The high salicylic acid absorption ability of SA/Na^+REC-g-IA/AM hydrogel film may be attributed to more quantity hydrophilic groups, the slight network of cross-section. The gradual penetration of water produces swelling to form a hydrated gel through which salicylic acid has to pass by dissolution and diffusion across the ever-increasing diffusional pathway length (Pongjanyakul et al., 2010). Fig. 7 gives the release behavior for salicylic acid in vitro of SA and SA/Na^+REC-g-IA/AM hydrogel film. Fig. 7 shows that all films have burst release in the first 12 h and then slow constant release but with different rates. SA/Na^+REC-g-IA/AM hydrogel film shows slower release in comparison to pure SA film. It is generally known that the drug release from hydrophilic matrices is a complex interaction between swelling, diffusion and erosion (Ding et al., 2012; Munday & Cox, 2000). SA/Na^+REC-g-IA/AM hydrogel film is lightly crosslinked network of hydrophilic polymer chains, which has a high degree of water uptake capacity and a small degree of erosion. It can create greater tortuosity of water-filled channel and then slower salicylic acid diffusion occurs from the hydrogel film

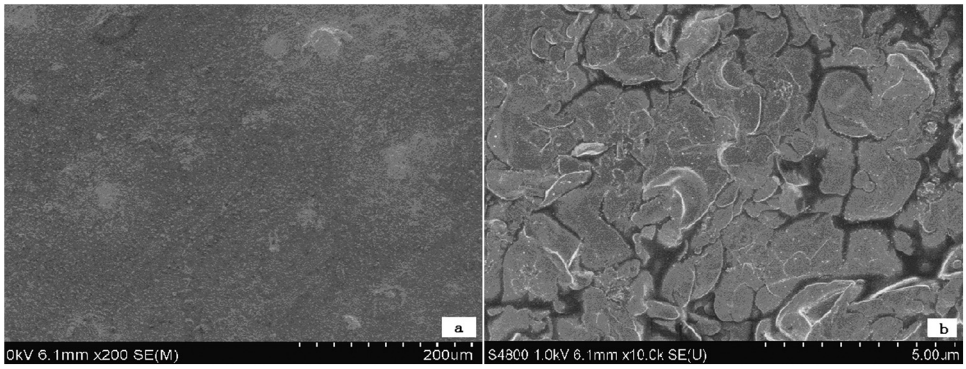

Fig. 6. SEM photographs of SA/Na^+REC-g-IA/AM hydrogel film. ((a) 200 times; (b) 10,000 times).

Table 1
Tensile strength and elongation value of SA and SA/Na⁺REC-g-IA/AM films

Samples	Dry film				Wet film			
	Tensile strength (MPa)	Standard deviation	Elongation value (%)	Standard deviation	Tensile strength (MPa)	Standard deviation	Elongation value (%)	Standard deviation
SA film	11.2	1.0392	33.7	0.0992	2.3	0.7239	13.4	0.0743
Hydrogel film	15.3	1.0006	62.3	0.1071	5.7	1.5716	30.6	0.3573

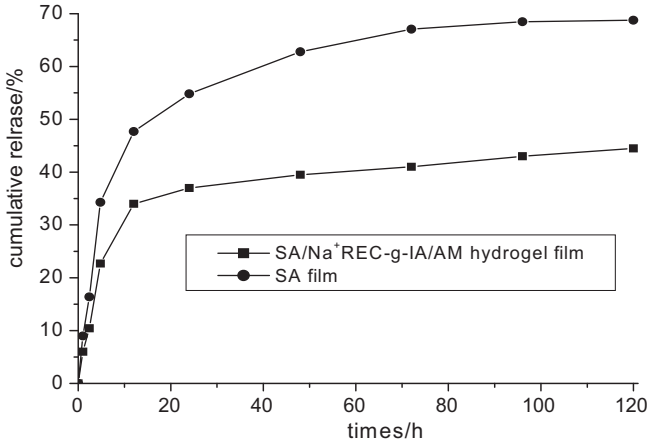

Fig. 7. Salicylic acid release in vitro studies of SA and SA/Na⁺REC-g-IA/AM films

(Ding et al., 2012; Munday & Cox, 2000; Yue et al., 2009). So it is certain that SA/Na⁺REC-g-IA/AM hydrogel film has excellent drug-controlled release properties. The Ritger–Peppas equation is the most commonly used to suggest two independent mechanisms of drug transport: Fickian diffusion and a case-II transport. To assess the possible mechanism of salicylic acid release, the data were fitted according to the Ritger–Peppas equation (Munday & Cox, 2000; Pongjanyakul et al., 2010; Yue et al., 2009).

$$\frac{M_t}{M_\infty} = kt^n \quad (5)$$

where M_t corresponds to the amount of drug released at time t; M_∞ is the total amount of drug released at infinite time; M_t/M_∞ is the fraction of drug released; t is the release time; k is a constant incorporating the structural and geometrical characteristics of the release device; n is the release exponent indicating the type of drug release mechanism. The values of n were obtained by linear regression analysis. For a swellable release system, $n < 0.45$, $0.45 < n < 0.89$ and $n > 0.89$ indicated a Fickian diffusion, a non-Fickian diffusion and a case-II transport, respectively (Munday & Cox, 2000; Pongjanyakul et al., 2010; Yue et al., 2009). The release exponent n of SA film and SA/Na⁺REC-g-IA/AM hydrogel film were 0.3980 ($r = 0.9413$) and 0.3867 ($r = 0.9266$), which were all lower than 0.45, indicating that the salicylic acid release mechanism followed Fickian diffusion.

4. Conclusions

SA/Na⁺REC-g-IA/AM hydrogel film was prepared via solution polymerization. The optimal content of Na⁺REC, KPS, NMBA and the ratio of IA to AM were 2 wt%, 0.8 wt%, 0.38 wt% and 4, respectively. XRD, TEM and SEM showed that the hydrogel film exhibited intercalative structure and coarse surface. The mechanism of graft copolymerization was discussed. The tensile strength and the elongation value of SA/Na⁺REC-g-IA/AM dry hydrogel film are found to be 15.3 MPa and 62.3%, respectively, which makes hydrogel film qualified for skin application. A slower and more continuous release of salicylic acid were shown from the in vitro drug-controlled release studies for SA/Na⁺REC-g-IA/AM composite hydrogel film, in comparison with SA film. The salicylic acid release of SA/Na⁺REC-g-IA/AM hydrogel film followed Fickian diffusion.

Acknowledgements

This work is supported by the National Natural Science Foundation of China under Grant (No. 50573046), the Shaanxi Province Education Commission Foundation No. 12JK0610, Xianyang Science and Technology Bureau Foundation No. 2011k05-05, Xianyang Normal University Foundation No. 10XSYK103 and College students' innovative projects of Xianyang Teacher's College No. 2013036.

References

Balakrishnan, B., Mohanty, M., Umashankar, P. R., & Jayakrishnan, A. (2005). Evaluation of an in situ forming hydrogel wound dressing based on oxidized alginate and gelatin. *Biomaterials*, *26*, 6335–6342.

Ding, J., He, R., Zhou, G., Tang, C., & Yin, C. (2012). Multilayered mucoadhesive hydrogel films based on thiolated hyaluronic acid and polyvinylalcohol for insulin delivery. *Acta Biomaterialia*, *8*, 3643–3651.

Bardajee, G. R., Pourjavadi, A., Soleyman, R., & Sheikh, N. (2008). Irradiation mediated synthesis of a superabsorbent hydrogel network based on polyacrylamide grafted onto salep. *Nuclear Instruments and Methods in Physics Research B*, *266*, 3932–3938.

Bunsow, J., & Johannsmann, D. (2008). Electrochemically produced responsive hydrogel films: Influence of added salt on thickness and morphology. *Journal of Colloid and Interface Science*, *326*, 61–65.

Deligkaris, K., Tadele, T. S., Olthuis, W., & van den Berg, A. (2010). Hydrogel-based devices for biomedical applications. *Sensors and Actuators B: Chemical*, *147*, 765–774.

Lanthong, P., Nuisin, R., & Kiatkamjornwong, S. (2006). Graft copolymerization, characterization, and degradation of cassava starch-g-acrylamide/itaconic acid superabsorbents. *Carbohydrate Polymers*, *66*, 229–245.

Montero, L., Gabriel, G., Guimerà, A., Villa, R., Gleason, K. K., & Borrós, S. (2012). Increasing biosensor response through hydrogel thin film deposition. *Influence of Hydrogel Thickness Vacuum*, *27*, 2102–2104.

Li, Z. H., Jiang, W. T., & Hong, H. L. (2008). An FTIR investigation of hexadecyltrimethylammonium intercalation into rectorite. *Spectrochimica Acta Part A: Molecular and Biomolecular Spectroscopy*, *71*, 1525–1534.

Liu, B. Z., Deng, Y. H., Hu, X. B., Gao, Z. Q., & Sun, C. (2012). Electrochemical sensing of trichloroacetic acid based on silver nanoparticles doped chitosan hydrogel film prepared with controllable electrodeposition. *Electrochimica Acta*, *76*, 410–415.

Mandal, B. B., Ghosh, B., & Kundu, S. C. (2011). Non-mulberry silk sericin/poly (vinyl alcohol) hydrogel matrices for potential biotechnological applications. *International Journal of Biological Macromolecules*, *49*, 125–133.

Kokabi, M., Sirousazar, M., & Hassan, Z. M. (2007). PVA–clay nanocomposite hydrogels for wound dressing. *European Polymer Journal*, *43*, 773–781.

Munday, D. L., & Cox, P. J. (2000). Compressed xanthan and karaya gum matrices: hydration, erosion and drug release mechanisms. *International Journal of Pharmaceutics*, *203*, 179–192.

Murakami, K., Aoki, H., Nakamura, S., Nakamura, S.-i., Takikawa, M., Hanzawa, M., Kishimoto, S., Hattori, H., Tanaka, Y., Kiyosawa, T., Sato, Y., & Ishihara, M. (2010). Hydrogel blends of chitin/chitosan, fucoidan and alginate as healing-impaired wound dressings. *Biomaterials*, *31*, 83–90.

Roy, N., Saha, N., Kitano, T., & Saha, P. (2012). Biodegradation of PVP–CMC hydrogel film: a useful food packaging material. *Carbohydrate Polymers*, *89*, 346–353.

Monvisade, P., & Siriphannon, P. (2009). Chitosan intercalated montmorillonite: preparation, characterization and cationic dye adsorption. *Applied Clay Science*, *42*, 427–431.

Pereira, R., Carvalho, A., Vaz, D. C., Gil, M. H., Mendes, A., & Bártolo, P. (2013). Development of novel alginate based hydrogel films for wound healing applications. *International Journal of Biological Macromolecules*, *52*, 221–230.

Shen, L., & He, P. L. (2007). An electrochemical immunosensor based on agarose hydrogel films for rapid determination of ractopamine. *Electrochemistry Communications*, *9*, 657–662.

Smitha, B., Sridha, S. R., & Khan, A. A. (2005). Chitosan–sodium alginate polyion complexes as fuel cell membranes. *European Polymer*, *41*, 1859–1866.

Teli, S. B., Gokavi, G. S., & Aminabhavi, T. M. (2007). Novel sodium alginate-poly(N-isopropylacrylamide) semi-interpenetrating polymer network membranes for pervaporation separation of water + ethanol mixtures. *Separation and Purification Technology*, *56*, 150–157.

Pongjanyakul, T., Priprem, A., & Puttipipatkhachorn, S. (2010). Investigation of novel alginate magnesium aluminum silicate microcomposite films for modified-release tablets. *Journal of Controlled Release*, *107*, 343–356.

Yoshimura, T., Uchikoshi, I., Yoshiura, Y., & Fujioka, R. (2005). Synthesis and characterization of novel biodegradable superabsorbent hydrogels based on chitin and succinic anhydride. *Carbohydrate Polymers*, *61*, 322–326.

Wang, X. Y., Du, Y. M., Luo, J. W., Lin, B. F., & John, F. (2007). Kennedy. Chitosan/organic rectorite nanocomposite films: Structure, characteristic and drug delivery behaviour. *Carbohydrate Polymers*, *69*, 41–49.

Wang, W. B., & Wang, A. Q. (2009). Preparation, characterization and properties of superabsorbent nanocomposites based on natural guar gum and modified rectorite. *Carbohydrate Polymers*, *77*, 891–897.

Wang, X. Y., Strand, S. P., Du, Y. M., & Vårum, K. M. (2010). Chitosan–DNA–rectorite nanocomposites: effect of chitosan chain length and glycosylation. *Carbohydrate Polymers*, *79*, 590–596.

Yang, L. L., Liang, G. Z., Zhang, Z. P., He, S. B., & Wang, J. H. (2009). Sodium alginate/Na^+Rectorite composite films: preparation, characterization, and properties. *Journal of Applied Polymer Science*, *114*, 1235–1240.

Yang, L. L., Ma, X. Y., & Guo, N. N. (2012). Sodium alginate/ Na^+-rectorite composite microspheres: preparation, characterization, and dye adsorption. *Carbohydrate Polymers*, *90*, 853–858.

Yue, Y. M., Sheng, X., & Wang, P. X. (2009). Fabrication and characterization of microstructured and pH sensitive interpenetrating networks hydrogel films and application in drug delivery field. *European Polymer Journal*, *45*, 309–315.

Zhao, Q. S., Ji, Q. X., Xing, K., Li, X. Y., Liu, C. S., & Chen, X. G. (2009). Preparation and characteristics of novel porous hydrogel films based on chitosan and glycerophosphate. *Carbohydrate Polymers*, *76*, 410–416.

Zhao, X. F., Li, Z. J., Wang, L., & La, X. J. (2008). Synthesis, characterization and adsorption capacity of crosslinked starch microspheres with *N*,*N*′-methylene bisacrylamide. *Journal of Applied Polymer Science*, *109*, 2571–2575.

Zhou, C. J., & Wu, Q. L. (2011). A novel polyacrylamide nanocomposite hydrogel reinforced with naturalchitosan nanofibers. *Colloids and Surfaces B: Biointerfaces*, *84*, 155–162.